Journal of Materials Chemistry A

Accepted Manuscript

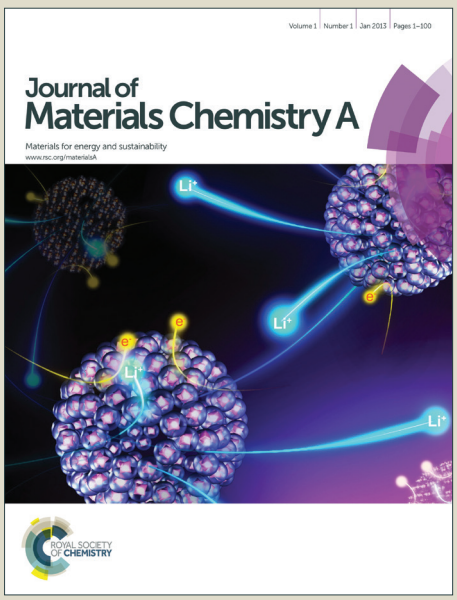

ROYAL SOCIETY OF CHEMISTRY

www.rsc.org/materialsA

Journal Name

RSCPublishing

COMMUNICATION

Ultrasmall palladium nanoparticles supported on amine-functionalized SBA-15 efficiently catalyze hydrogen evolution from formic acid

Cite this: DOI: 10.1039/xoxxooooox

Received ooth January 2012,
Accepted ooth January 2012

DOI: 10.1039/xoxxooooox

www.rsc.org/

K. Koh[a], J.-E. Seo[d], J.H Lee[d], A. Goswami [ab,*], C.W.Yoon [de,*]and T. Asefa[abc,*]

The success of the so-called "hydrogen economy" for large-scale applications will ultimately depend on efficient and sustainable production, storage and distribution of hydrogen. Owing to its low toxicity, high volumetric H_2 storage capacity and availability both from renewable resources (e.g., biomass) as well as non-renewable resources (e.g., fossil fuel feedstocks), formic acid is one of the most favorable chemical hydrogen storage media for large-scale energy storage applications. However, for FA to become a viable hydrogen storage medium, efficient catalysts that enable it to release H_2 at low cost are necessary. Herein we report a facile synthetic route to amine-functionalized nanoporous silica-supported ultrasmall Pd nanoparticles (SBA-15-Amine/Pd) that are highly active catalysts for formic acid dehydrogenation, producing hydrogen at ambient temperature with a high turn-over-frequency (TOF) of 293 h^{-1}—which is among the highest TOFs ever reported for the reaction by a heterogeneous catalyst. We also show that the material is easily recyclable multiple times, without losing its catalytic activity. So, the catalyst we developed might contribute to some of the solutions of our sustainability challenges.

Given the current energy landscape, where the consumption of fossil fuels continues to rise while the negative environmental impacts associated with burning fossil fuels continues unabated, the search for alternative, benign and sustainable energy sources is a burgeoning interest. In this context, hydrogen—as one of the most promising clean energy carriers—can play pivotal roles to meet these challenging issues facing the world, as already successfully demonstrated with clean hydrogen-fed fuel cell technologies.[1-4] Despite the progress made since the 1970s, when the term "hydrogen economy" was coined by Bockris,[2] it has become apparent that the ultimate success of the hydrogen-based energy cycle for large scale applications heavily hinges on efficient, large-scale production, storage, and distribution of hydrogen. In particular, the development of safe and reversible hydrogen storage systems is a key technical issue that must be fully addressed to successfully realize an "ideal" hydrogen economy.[5-7]

Because of its low toxicity and high availability both from renewable resources (e.g., biomass) as well as non-renewable resources (e.g., fossil-feedstock), formic acid (FA) has recently attracted significant attention for its potential as favorable chemical hydrogen storage medium for large-scale energy storage applications.[8-9] FA's appeal as favorable hydrogen carrier also stems from the fact that it has a high volumetric H_2 storage capacity of 53 g/L, which is suitable for many on-board energy applications.[10] Moreover, FA can be dehydrogenated to produce the hydrogen it carries under ambient conditions, making it auspicious for direct utilization within hydrogen-fed polymer electrolyte membrane-based fuel cells (PEMFCs).

For FA to be used as a viable hydrogen storage medium though, efficient catalysts that enable it to generate H_2 at low cost are critically needed. In recent years, various homogeneous catalysts based on metals such as Ru[11-14] and Ir[15] and heterogeneous catalysts including AuPd/C,[16] AgPd[17], CoAuPd/C,[18] Pd/C_3N_4[19,20]for dehydrogenation of FA have been reported. Generally, homogeneous catalysts are highly active and exhibit higher turnover frequencies (TOFs) than heterogeneous catalysts for many reactions including formic acid dehydrogenation. However, the heterogeneous catalysts are generally advantageous over homogeneous ones in terms of recoverability of the spent-catalysts from the reaction mixtures.[21] By immobilizing homogeneous catalysts onto solid support materials, the benefits attainable by both types of catalysts can sometimes be realized. This approach of 'heterogenization of homogeneous catalysts' can also be successfully applied for catalytically active ultrasmall metallic nanoclusters, which have been increasingly become promising catalysts for formic acid dehydrogenation.[22-26] Furthermore, functional groups such as amines could easily be supported on the surfaces of such heterogeneous catalysts to serve as interaction sites for supported metallic nanoclusters and serve as co-catalytic species, which in the case of FA-dehydrogenation can

function as deprotonation sites for FA molecules, synergistically assisting FA's catalytic dehydrogenation. This hypothesis, in conjunction with the recent success of other gold (Au) nanoparticles encapsulated in silica nanospheres[26] and Pd supported catalysts over materials such as silica microspheres[22] or metal-organic frameworks (MOFs)[24] for FA dehydrogenation, has prompted us to develop an efficient hybrid catalyst based on ultrasmall Pd nanoparticles (Pd NPs) supported on amine-functionalized mesoporous silica for FA dehydrogenation, as shown in Scheme 1.

First, SBA-15 type mesoporous silica was synthesized using soft templating-based, supramolecular self-assembly synthetic technique, as demonstrated by Zhao et al.[27] By using the residual surface silanols (≡Si-OH) located on the pore walls of SBA-15, the material was functionalized with organic functionalities, which were then utilized to anchor metal ions onto the surfaces of the nanoporous material.[28,29] In this current effort, primary amine groups were anchored on SBA-15 by grafting (3-aminopropyl)triethoxysilane (APTES) onto the surfaces of SBA-15, producing a material denoted as SBA-15-Amine (Scheme 1). Then, Pd^{2+} ions were supported onto the surfaces of SBA-15-Amine by mixing the latter with ammonical palladium solution ($Pd(NH_3)_4Cl_2$).[30] Subsequent reduction of the resulting material using H_2/N_2 mixture (1:9 v/v) at 250 ºC for 3 h afforded SBA-15-Amine-suppported Pd NPs (denoted hereafter as SBA-15-Amine/Pd) that are highly catalytically active for FA dehydrogenation (see detailed experiment in supporting information).

The structures and morphology of SBA-15-Amine/Pd were first analyzed by high-resolution transmission electron microscopy (HRTEM) and high-angle annular dark-field scanning transmission electron microscopy (HAADF-STEM). The Pd nanoparticles in SBA-15-Amine/Pd were found to be ultrasmall, having an average size of 1.9 nm (Figures 1a-b). In contrast, the unmodified SBA-15/Pd prepared under otherwise identical synthetic conditions afforded relatively bigger Pd NPs (Figures 1c-d). The latter is not surprising since ultrasmall Pd NPs are often too difficult to obtain with conventional reduction methods employing $NaBH_4$ and/or without capping agents because they tend to aggregate easily due to their relatively high surface energies (*vide infra*). In our other control experiment, the Pd NPs formed following the reduction of the ammonical Pd(II) species in the absence of SBA-15-Amine were also, unsurprisingly, significantly bigger in size, having particle sizes as high as 150 nm (Figure S2). Thus, the amine functional groups inside the mesoporous silica and their ability to stabilize the Pd NPs must have played important roles in keeping the Pd NPs quite small during reduction of Pd^{2+} ions under H_2 at 250 ºC. The amounts of Pd in the SBA-15-Amine/Pd and SBA-15/Pd, as characterized by ICP-AES, were found to be identical (0.32 mmol/g_{cat}, 3.4 wt. %). On the basis of other previous report,[31] it is conceivable that the amine functional groups grafted in our SBA-15-Amine/Pd could serve as Brønsted basic sites, facilitating the deprotonation of FA into formate intermediate, while the ultrasmall Pd NPs around them catalytically activate the C-H bonds of the resulting formate species. Besides this, the amine groups help with both the formation as well as stabilization of the ultrasmall Pd NPs (or protect them from undergoing aggregation during the catalytic reactions (see below)).

Furthermore, the amine groups supported onto the SBA-15 can donate electron density to Pd, thereby enhancing the Pd's catalytic activity of towards FA dehydrogenation.[31] To elucidate this possible electronic effect of the amine groups on Pd, X-ray photoelectron spectroscopy (XPS) was employed to analyze the materials and the results are displayed in Figure 2 and Figures S2 and S3. As depicted in the spectra, while the peaks corresponding to Pd(0) in SBA-15/Pd with maxima are centered at 341.0 eV ($3d_{3/2}$ state) and 335.8 eV ($3d_{5/2}$ state),[32] the corresponding peaks in the case of SBA-15-Amine/Pd are shifted into lower binding energies of 340.1 eV and 335.0 eV, respectively. This is likely due to the interaction between Pd NPs and amine groups in SBA-15-Amine/Pd; *i.e.*, the amine groups donating some electron density to Pd NPs and producing electron- rich Pd centers with lower binding energies. These electronically perturbed Pd centers in SBA-15-Amine/Pd could thus be partly responsible for the material's improved catalytic activity towards FA dehydrogenation compared with that of SBA-15/Pd (*vide infra*). It is worth-adding here that the Pd_{3d} spectra for both materials showed two small peaks corresponding to Pd^{2+} centered at 343.2 eV and 337.9 eV, respectively, clearly indicating negligible presence of Pd^{2+} species.

Next, we evaluated the catalytic activities of SBA-15-Amine/Pd, SBA-15-Amine, SBA-15/Pd, and bare Pd NPs toward FA dehydrogenation at room temperature in the absence of external bases using the set-up shown in Figure S4. As illustrated in Figure 3, among these various materials we investigated SBA-15-Amine/Pd showed superior activity towards FA dehydrogenation. The rate and amount of total H_2-release from FA over SBA-15-Amine/Pd were quite good with an initial TOF of 300 h^{-1} in 10 min, which is among the highest TOF for FA dehydrogenation compared with the TOF values previously reported for other heterogeneous catalysis under ambient condition without bases.[11-20] The TOFs of recently developed heterogeneous catalysts without additives at ambient temperature are compared in Table S1 entries 1-6 and Figure S5. It is also valuable to compare with recent most active palladium catalyst, Pd/MSC-30, under ambient condition that employed sodium formate along with formic acid in the reaction (Table S1, entry 7)[33] The control materials, SBA-15/Pd and Pd NPs, showed only little

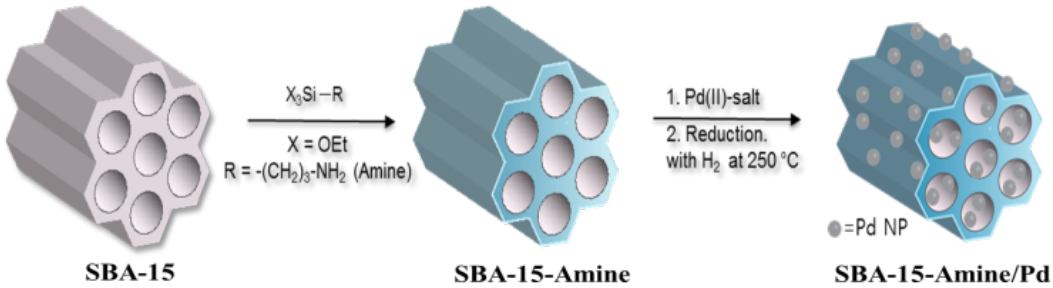

Scheme 1. A synthetic scheme employed for making ultrasmall Pd nanoparticles supported on amine-functionalized SBA-15 mesoporous silica, which can efficiently catalyze formic acid (FA) dehydrogenation.

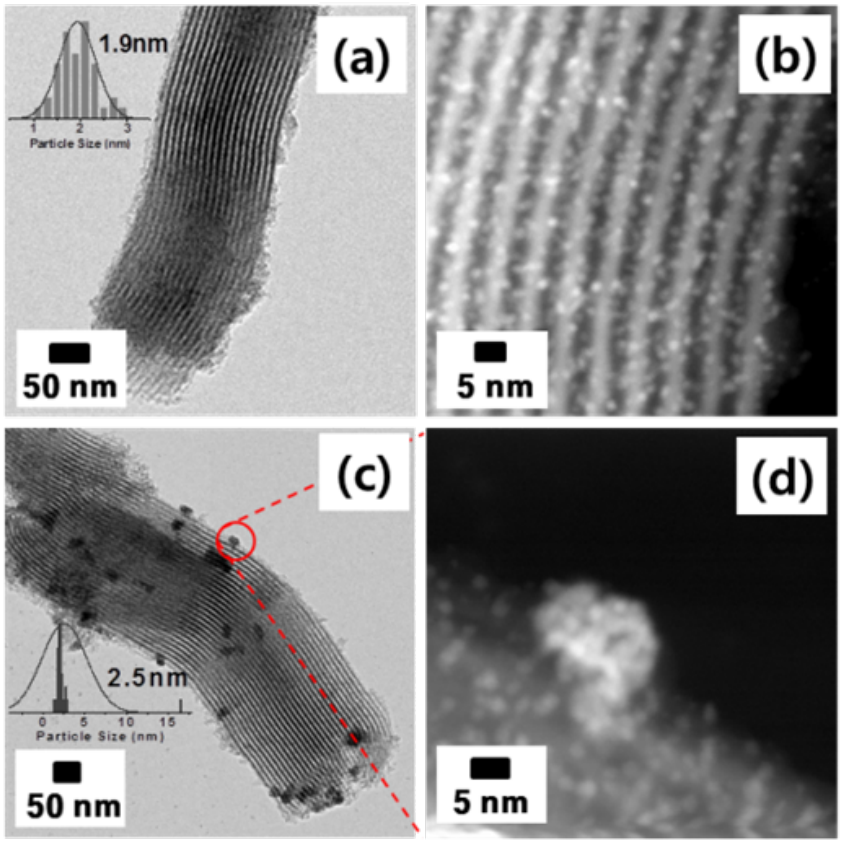

Figure 1. TEM (a) and STEM (b) images of SBA-15-Amine/Pd. TEM (c) and STEM (d) images of SBA-15/Pd. The insets show the size distributions of the particles obtained from the TEM images.

catalytic activity, again supporting that the amine functional groups in SBA-15-Amine/Pd play a pivotal role in accelerating FA dehydrogenation. It is also worth noting that the mesoporous silica material has no activity on its own towards the reaction.

To further scrutinize the potential roles of the covalently tethered amine functional groups in the catalytic activity of the material towards FA dehydrogenation, we carried additional controlled experiments by using the physical mixtures of SBA-15/Pd and various quantities of *n*-propylamine (PA) as catalyst. Compared with SBA-15/Pd, the physical mixture of SBA-15/Pd and 0.1 mmol of PA showed an increased catalytic activity (Figures 3a and b). Note that the amount of amine or PA added is 0.1 mmol, which is almost equal to that covalently tethered amines in SBA-15-Amine/Pd. Upon addition of higher amount (5 mmol) of PA (Figure 3a, indicated with pink triangles), the corresponding activity increased slightly, but was still significantly lower than that obtained with SBA-15-Amine/Pd. Nevertheless, these results strongly imply that the added amine clearly acted as a Brønsted base, helping the deprotonation of FA. The results also suggest that the amine functional groups on the pore walls of SBA-15-Amine/Pd play multiple functions; *i.e.*, effectively deprotonating FA, besides

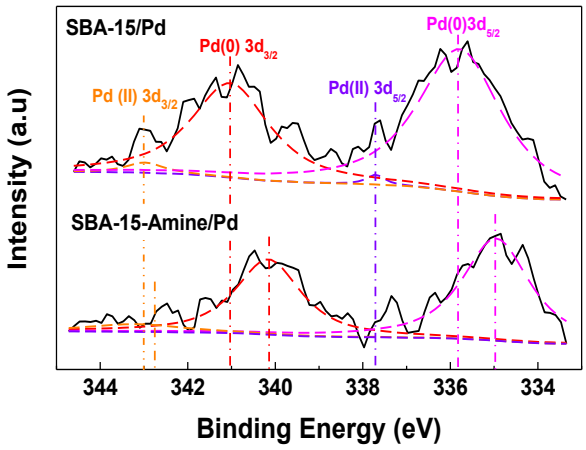

Figure 2. The high resolution Pd_{3d} peaks in the XPS spectra of SBA-15-Amine/Pd and SBA-15/Pd.

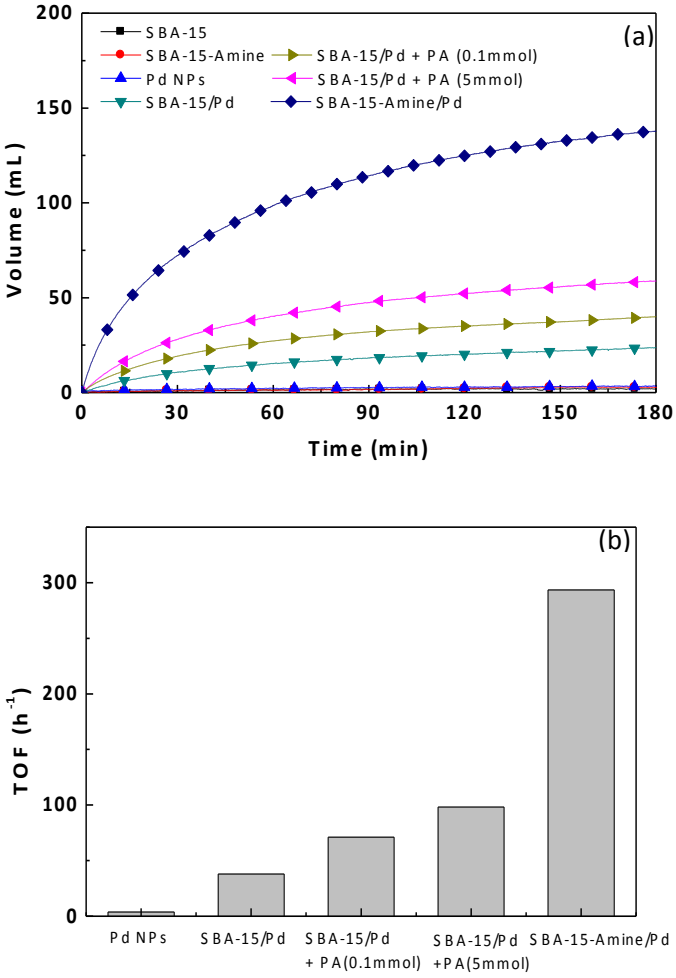

Figure 3. FA dehydrogenation catalyzed by the various materials synthesized and investigated here. (a) The volume of total gases produced versus time (min) curves. (b) TOFs at 10 min calculated based on the mol of Pd in the materials (catalysts). Reaction condition: 10 mL of 1 M FA was stirred with 50 mg of a desired catalyst (16 μmol of palladium) at room temperature at 300 rpm.

allowing the synthesis of well-dispersed, electron rich, and catalytically active ultrasmall Pd NPs for FA. As a result, the rate of dehydrogenation of FA over the SBA-15-Amine/Pd is much more enhanced.

FA is known to decompose *via* two possible pathways: (1) dehydrogenation ($HCOOH \rightarrow H_2 + CO_2$) and dehydration ($HCOOH \rightarrow H_2O + CO$).[34] To obtain better FA dehydrogenation systems for hydrogen production, catalysts that favor the former and suppress the latter are unquestionably preferred. This is because the second (dehydration) process does not produce H_2, not to mention it forms CO–a common poison for many catalysts, including the Pt catalysts typically used in hydrogen-fed PEMFCs.[35-39] To examine the selectivity of the overall reaction to the one leading to the desired product, *i.e.*, H_2, as defined as [moles of H_2/moles of (H_2 +CO)]×100, FT-IR spectroscopy was employed to detect CO directly (Figure S6). The FT-IR spectrum obtained using SBA-15-Amine/Pd after 50 min gave a doublet peak located at ca. 2300 cm^{-1}, indicating the evolution of CO_2. The peak at ca. 2100 cm^{-1} corresponding to CO was barely observable, strongly suggesting that H_2 selectivity is close to ca. 100 %.

Recyclability studies of the catalytic material were additionally carried out for SBA-15-Amine/Pd. The result revealed that the catalyst was reusable at least six times without losing its activity (Figure 4). Interestingly, the TOFs were, in fact, found to increase after the 1st run becoming nearly identical for 2nd – 6th runs, reaching values as high as 377 h^{-1}. Consistent with these results, the TEM images of SBA-15-Amine/Pd revealed no appreciable change in the structure of mesoporous silica even following completion of 6th catalytic recycle run. Moreover, the size of Pd NPs also remained unchanged (Figure 5). The improved performance of the recycled catalysts particularly after the first cycle can be attributed to the reductive environment (due to the H_2 produced by the reaction) that the catalyst is exposed to during the catalytic reactions, which can convert any surface-oxidized PdO possibly present on the original catalyst back to the catalytically active Pd-NPs. The condition which can convert any possibly oxidized PdO back to catalytic be active Pd and also prevents the Pd NPs from undergoing oxidation and losing their activity. Finally, to determine possible leaching of Pd from SBA-15-Amine/Pd during the reactions, the supernatant obtained after 150 min was examined by ICP-AES. The amount of Pd in the supernatant was found to be only ca. 10 ppm, indicating that the Pd NPs remain supported on SBA-15-Amine/Pd during the dehydrogenation reaction. On the other hand, the amount of amine in the materials after 6th recycle, obtained based on analysis of atomic percentage of nitrogen on XPS (Table S2 and Figure S7), remains almost unchanged.

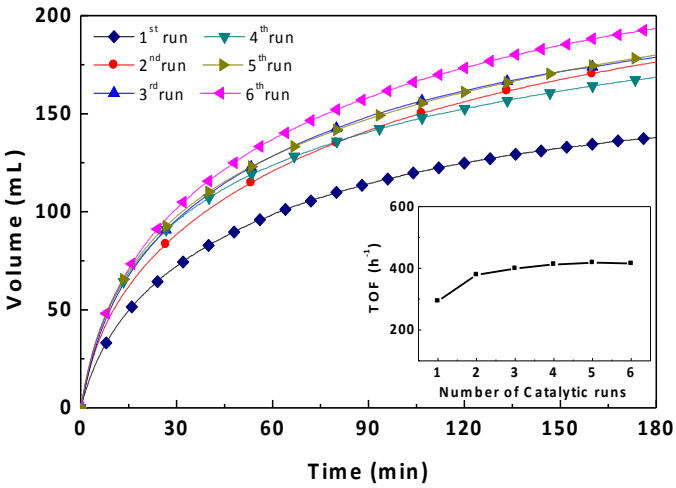

Figure 4. Recyclability results of SBA-15-Amine/Pd used in FA dehydrogenation: Volume (mL) of gas products (H_2 + CO_2) versus time (min). Inset shows a plot of initial TOFs versus catalytic recycle runs.

Journal Name

RSCPublishing

COMMUNICATION

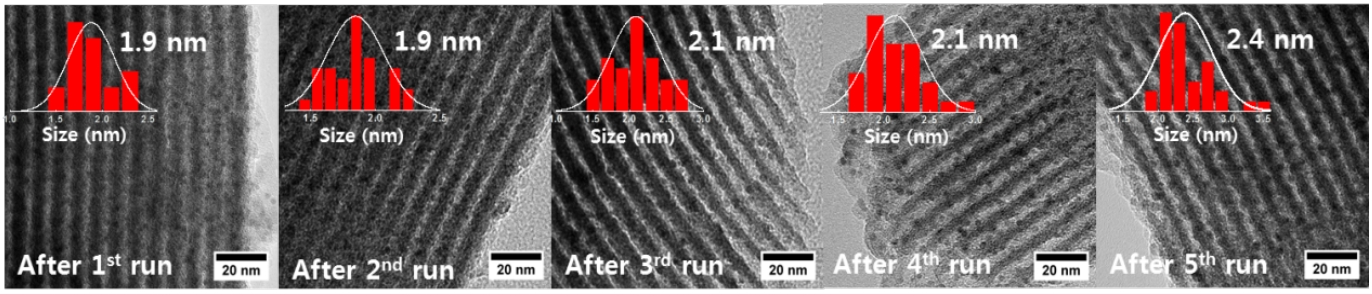

Figure 5. TEM images of spent SBA-15-Amine/Pd catalysts after each catalytic reaction cycle.

In conclusion, amine-functionalized SBA-15-supported ultrasmall Pd NPs are synthesized and shown to have excellent activity towards FA dehydrogenation at room temperature in the absence of any external base, giving an initial TOF of $293 h^{-1}$—one of the highest values reported so far for heterogeneous catalysts, to the best of our knowledge (Table S1 and Figure S5). Despite the difference in synthetic strategies, the support materials, the metals involved and the catalytic procedures used in our case and in some of the previous related works, based on the catalytic outcomes there appears to be the so-called "strong metal–molecular support interaction (SMMSI) reported by Yadav et al.[26] at play in our material as well, or is more likely to be responsible for the enhanced catalytic activities attained in it. But some other subtle metal-ligand interactions may have also additionally contributed to the higher catalytic activity in our case as compared with the non-ligand counterparts because: 1) the surface properties, the size of the metal-nanoparticles of the amine-grafted catalysts and non-amine catalysts like ours are quite different and 2) based on recently reported mechanistic details [31] as well as some of our ongoing work, we also believe, the supported amine groups play an additional role as a base.

Acknowledgements

T.A. acknowledges the partial financial support of the NSF (DMR-0968937 and NanoEHS-1134289) for the work in his lab.

Notes and references

[a] *Department of Chemistry and Chemical Biology, Rutgers, The State University of New Jersey, 610 Taylor Road, Piscataway, New Jersey 08854, USA.E-mail: tasefa@rci.rutgers.edu; agoswami@rci.rutgers.edu*

[b] *Department of Chemical and Biochemical Engineering, Rutgers, The State University of New Jersey, 98 Brett Road, Piscataway, New Jersey 08854, USA*

[c] *Institute for Advanced Materials, Devices and Nanotechnology (IAMDN), Rutgers, The State University of New Jersey, 607 Taylor Road, Piscataway, New Jersey 08854, USA.*

[d] *Fuel Cell Research Center, Korea Institute of Science and Technology, Hwarangno14-gil 5, Seongbuk-gu, Seoul 136-791, Republic of Korea. E-mail: cwyoon@kist.re.kr*

[e] *Department of Clean Energy and Chemical Engineering, University of Science and Technology, Daejeon, Republic of Korea.*

† Electronic Supplementary Information (ESI) available: Detailed experimental procedures, TEM, FT-IR, TOF calculation data. See DOI: 10.1039/c000000x/

1. A. Haryanto, S. Fernando, N. Murali, S. Adhikari, *Energy Fuels* 2005, **19**, 2098–2106.
2. J. O.M. Bockris, *Science* 1972, **176**, 1323.
3. Hydrogen and Fuel Cells. Fundamentals, Technologies and Applications, Edited by D. Stolten, Wiley-VCH, Weinheim 2010.
4. M. Yadav, Q. Xu, *Energy Environ. Sci.*, 2012, **5**, 9698-9725.
5. J. Yang, A. Sudik, C. Wolverton, D. J. Siegel, *Chem. Soc. Rev.*, 2010, **39**, 656–675.
6. X. Zou, X. Huang, A. Goswami, R. Silva, B. R. Sathe, T. Asefa, *Angew. Chem. Int. Ed.*, 2014, **53**, 4372–4376
7. G. Xie, K. Zhang, B. Guo, Q. Liu, Liang Fang, J. R. Gong, *Adv. Mater.* 2013, **25**, 3820–3839.
8. S. Dapía, V. Santos, Parajó, *Biomass Bioenergy* 2002, **22**, 213–221
9. W. Reutemann, H. Kieczka, in *Ullmann's Encyclopedia of Industrial Chemistry*, Wiley-VCH, Weinheim, 2011.
10. M. Grasemann, G. Laurenczy, *Energy Environ. Sci.* 2012, **5**, 8171–8181.
11. B. Loges, A. Boddien, H. Junge, M. Beller, *Angew. Chem. Int. Ed.* 2008, **47**, 3962–3965;
12. S. Adhikari, S. Fernando, A. Haryanto, *Int. J. Hydrogen Energy*, 2007, **32**, 2875–2880;

13. Y. Gao, J. K. Kuncheria, H. A. Jenkins, R. J. Puddephatt, G. P. A. Yap, *J. Chem. Soc., Dalton Trans*. 2000, 3212–3217.
14. S. Adhikari, S. Fernando, A. Haryanto, *Catal. Today*. 2007, **129**, 355–364.
15. Y. Himeda, Green Chem. 2009, **11**, 2018–2022.
16. Ö. Metin, X. Sun, S. Sun, *Nanoscale* 2013, **5**, 910–912.
17. K. Tedsree, T. Li, S. Jones, C. W. A. Chan, K. M. K. Yu, P. A. J. Bagot, E. A. Marquis, G. D. W. Smith, S. C. E. Tsang, *Nat. Nanotechnol.* 2011, **6**, 302–307.
18. Z.-L. Wang, J.-M. Yan, Y. Ping, H.-L. Wang, W.-T. Zheng, Q. Jiang, *Angew. Chem. Int. Ed.* 2013, **52**, 4406–4409.
19. Y.-Y. Cai, X,-H. Li, Y.-N. Zhang, X. Wei, K.-X. Wang, J.-S. Chen, *Angew. Chem. Int. Ed.* 2013, **52**, 11822–11825
20. J. H. Lee, J. Ryu, J. Y. Kim, S.-W. Nam, J. H. Han, T.-H. Lim, S. Gautam, K. H. Chae, C. W. Yoon, *J. Mater. Chem. A* 2014, **2**, 9490–9495.
21. D. J. Cole-Hamilton, *Science* 2003, **299**, 1702-1706.
22. Y. Zhao, L. Deng, S.-Y. Tang, D.-M. Lai, B. Liao, Y. Fu, Q.-X. Guo, *Energy Fuels* 2011, **25**, 3693–3697
23. M. Martis, K. Mori, K. Fujiwara, W.-S. Ahn, H. Yamashita, *J. Phys. Chem. C* 2013, **117**, 22805–22810
24. J. Vicente, J. Ereña, L. Oar-Arteta, M. Olazar, J. Bilbao, and A. G. Gayubo, *Ind. Eng. Chem. Res.*, 2014, **53**, 3462–3471
25. W. Zhu, R. Michalsky, Ö. Metin, H. Lv, S. Guo, C. Wright, X. Sun, A. A. Peterson, S. Sun, *J. Am. Chem. Soc.* 2013, **135**, 16833–16836.
26. M. Yadav, T. Akita, N. Tsumoriab, Q. Xu, *J. Mater. Chem*., **2012**, *22*, 12582–12586.
27. D. Zhao, J. Feng, Q. Huo, N. Melosh, G. H. Fredrickson, B. F. Chmelka, G. D. Stucky, *Science* 1998, **279**, 548–552.
28. F. Hoffmann, M. Cornelius, J. Morell, M. Froba, *Angew Chem. Int. Ed.* 2006, **45**, 3216–3251
29. E. L. Margelefsky, R. K. Zeidan, M. E. Davis, *Chem. Soc. Rev.* 2008, **37**, 1118–1126.
30. C. Li, Q. Zhang, Y. Wang, H. Wan, *Catal. Lett.* 2008, **120**, 126–136.
31. K. Mori, M. Dojo, H. Yamashita, *ACS Catal.* 2013, **3**, 1114–1119.
32. G. Kumar, J. R. Blackburn, R. G. Albridge, W. E. Moddeman, M. M. Jones, *Inorg. Chem.* 1972, **11**, 296–300.
33. Q. Zhu, N. Tsumori, Q. Xu, *Chem. Sci.*, 2014, **5**, 195-199.
34. N. Akiya, P. E. Savage, *AIChE J.* 1998, **44**, 405–415.
35. B. Winther-Jensen, K. Fraser, C. Ong, M. Forsyth, D. R. MacFarlane, *Adv. Mater.* 2010, **22**, 1727–1730
36. G. A. Camara, E. A. Ticianelli, S. Mukerjee, S. J. Lee, J. McBreen *J. Electrochem. Soc.* 2002, **149**, A748–A753
37. A. Manasilp, E. Gulari, *Appl. Catal. B: Environ.* 2002, **37**, 17–25
38. J. S. Lee, S. Locatelli, S. T. Oyama, M. Boudart, *J. Catal.* 1990, **125**, 157–170
39. Q. Li, R. He, J.-A. Gao, J. O. Jensen, N. J. Bjerrum, *J. Electrochem. Soc*. **2003**, *150*, A1599–A1605.

Graphical Abstract:

Amine-functionalized mesoporous silica-supported ultrasmall Pd nanoparticles catalyze hydrogen evolution from formic acid at ambient temperature.